ALPHA DECAY BRANCHING RATIOS AND ITS POSSIBLE IMPLICATIONS REGARDING NUCLEAR STRUCTURE

A thesis submitted in the partial fulfillment of requirement for the award degree

Masters of Science

In

Physics

Submitted by

Gurvarinder

Roll no.-300804008

Under the esteemed guidance of

Dr. Manoj K. Sharma

(Associate professor)

School of physics and material science

Thapar University

PATIALA (PUNJAB)-147004

July 2010

DEDICATION

This dissertation work is dedicated to my wonderful parents, S.Parminderjit Singh and Mrs. Jaswinder Kaur, who have raised me to be the person I am today. They taught me that the best kind of knowledge to have is that which is learnt for its own sake and that the largest task can be accomplished if it is done one step at a time.

I also thank my beloved grandparents, S.Bhupinder Singh and Mrs. Surjit Kaur, my maternal uncles Dr. Inderjit Singh and S. Jatinder Singh, maternal aunts Dr. Hardeep Kaur and Mrs. Prabhjot Kaur and my brothers Rupinder, Roopanjit, Tanveer and Japreet for their never ending moral support and prayers which always acted as catalyst in my academic life.

Finally this work is dedicated to all those who believe in richness of learning.

CERTIFICATE

This is to certify that Ms. Gurvarinder, Roll No. 300804008 has worked on this thesis report as a partial fulfillment for award of the degree of **MASTERS OF SCIENCE** in physics. I certify that the matter embodied in this report is of candidate's own record and not submitted to any other university in any part or full form for the award of such a degree.

(Dr. Manoj K. Sharma)

Supervisor

SPMS, Thapar University

Patiala.

Countersigned by:

Dr. O.P. Pandey
(Prof. & Head)

School of Physics and Materials Science,

Thapar University,

Patiala.

Dr. R.K. Sharma
(Dean of academic Affairs)

Thapar University,

Patiala.

Acknowledgement

I owe my deepest gratitude to **Dr. Manoj K. Sharma**, *my worthy supervisor*, who has been an inspiration during my research work. Without him, this thesis would not have been possible. I thank him for his patience and encouragement that carried me on through difficult times, and for his insights and suggestions that helped to shape my research skills. I express my sincere thanks to him for his valuable guidance in carrying out work under his effective supervision, encouragement and cooperation. His visionary thoughts have influenced me greatly. His dynamical attitude has empowered me with a zeal of energy to conquer the minor details of my research work.

I also thank **Dr. O. P. Pandey**, Professor and Head, School of Physics and Material Science for his support and providing facilities.

A special word of thanks to **Ms. Gudveen**, Research Scholars for the help and valuable suggestions whenever I needed out of her busy schedule.

Special thanks are due to Ekta, Nandini, Kiran, Gurvinder, Aman and all my classmates and the staffs at the School of Physics and Material Sciences for providing me a friendly atmosphere and encouraging me throughout this work.

I am deeply thankful to my Family, their moral support and patience has bared fruit through completion of this thesis.

Gurvarinder

Roll no. 300804008

ABSTRACT

In this dissertation work the α-branching ratios of ^{238}Pu, ^{242}Cm and ^{246}Cf are calculated in the framework of the decay cluster model (DCM) by taking into account angular momentum of the α-particle and the excitation probability of the residual daughter nucleus. This is done using two approaches, the unified fission approach within which the preformation probability of α-fragment is taken as unity and preformed cluster approach in which the appropriate values of preformation probabilities are used in calculations. The calculated α-transition branching ratios are in good agreement with the experimental data.

Table of Contents Page No.

LIST OF FIGURES

LIST OF TABLES

Chapter 1

Introduction

The composition of matter has puzzled philosophers for centuries and scientists for decades. Even today the mystery continues, as strange new particles are detected in high-energy accelerators used to probe the structure of matter. Various models proposed to explain the composition and mechanics in matter are useful in certain applications but invariably fall short for others.

The simplest view of the atomic nuclei is that they are composed of neutrons and protons, collectively called nucleons. Theoretical and experimental studies of nuclei revealed that the nucleons constituting them, are not distributed uniformly inside a nucleus. These studies proved the presence of “clusters” of nucleons in the nucleus and the participation of such clusters in nuclear reactions. Of all such clusters, the one formed by two protons and two neutrons is the most ubiquitous because of its high symmetry and binding energy. As is well known, this is referred to as the α-particle, although its properties inside the nucleus may not be the same as that of a free α-particle, owing to the action of the surrounding nucleons.

Some nuclei can spontaneously emit the α-particles. This phenomenon was discovered at the very beginning of the nuclear era and is known as the α-decay. It was not only historically first to be detected but it has led to most valuable information on nuclear structure and characteristics of nuclear reactions. The energy measurements of α-decay give information about nuclear binding energies and nuclear structure, the determination of half-lives give information about decay mechanism and the energy spectra of α-particles give information about the level scheme of the parent and daughter nucleus.

Many heavy nuclei, especially those of the naturally occurring series, decay through α-emission. Only exceedingly rarely does any other spontaneous radioactive

process result in the emission of nucleons; we do not, for example, observe deuteron emission as a natural decay process. There must therefore be a special reason for the nuclei to choose α-emission over other possible decay modes. Although the clusters heavier than α-particle are measured experimentally and observed theoretically during last three decades but the probability of emission of such clusters (heavier than α-particle and smaller than fission fragments) is extremely small as compared to α-decay.

1.1 Why α-decay occurs?

The α-decay process becomes increasingly important for heavy nuclei because the disruptive coulomb force increases with size at a faster rate (namely as Z^2) than does the specific nuclear binding force, which increases approximately as A. Therefore α-decay process can be attributed to the coulomb repulsion effect.

The α-particle acts as the agent for spontaneous carrying away of positive charges in order to stabalise a heavy nuclear system. When we call a process spontaneous we mean that some kinetic energy has suddenly appeared in the system for no apparent cause; this energy must come from a decrease in the mass of the system. The α-particle, because it is a very stable and tightly bound structure, has a relatively small mass as compared to the mass of its separate constituents. It is particularly favored as an emitted particle if we hope to have disintegration products as light as possible and thus get the largest possible release of kinetic energy in order to have maximum stability to the decaying nucleus..

For a typical α-emitter ^{232}U ($t_{1/2}$ = 72 y) we can compute from the known masses the energy release for various emitted particles. The table 1.1 [1] summarizes the results.

Table 1.1. Energy released during emission of various particles from ^{238}U nucleus.

Emitted Particle	Energy Released (MeV)	Emitted Particle	Energy Released
N(Neutron)	-7.26	^{4}He	+5.41
^{1}H	-6.12	^{5}He	-2.59
^{2}H	-10.70	^{6}He	-6.19
^{3}H	-10.24	^{6}Li	-3.79
^{3}He	-9.92	^{7}Li	-1.94

.

Of the particles mentioned in table 1.1 [1], spontaneous decay is energetically possible only for the α-particle. A positive disintegration energy also results for some slightly heavier particles than those listed above ^{8}Be, ^{12}C, ^{16}O, etc cluster shows such kind of behavior. However, the partial disintegration constant for emission of such heavy particles is normally vanishingly small compared with that for α-emission. Such decays are so rare that in practice they are difficult to observe and investigate. Although emergence and utilization of these heavy clusters is well understood in another subject of nuclear physics known as cluster radioactivity. In recent times a lot of work has been done on such heavy cluster masses which seem to have strong dependence on Q-value and shell closure of daughter nucleus alongwith significant contribution of deformation and orientation of emitted clusters from spherical / deformed parent nuclei of actinide region.

This suggests that if nucleus is to be recognized as an α-emitter it is not enough for α-decay to be energetically possible .The disintegration constant must also not be too small or else α-emission will occur so rarely that it may not be detected. With present techniques this means that the half-life must be less than about 10^{16} y. Most nuclei with A>190 are energetically unstable against α-emission but only one-half of them can meet these requirements.

1.2 Theory of α-decay

Historically the theory of alpha decay has developed through three stages. The first stage was characterized by a theoretical explanation of the global characteristics of the process: quantum mechanical barrier penetration. The emission of α-particles from some nuclei suggested that fully preformed α-particles exist in them, and their scarce appearance indicated that they are restrained by a potential barrier. The approach was independently and almost simultaneously given by Gamow [2] and by Condon and Gurney [3]. In Gamow's treatment, the alpha cluster was assumed to be "particle" present in the nucleus from the outset and the problem of clustering was not considered. Today we would say that this was a macroscopic theory. The solution of the problem was one of the first successes of quantum mechanics to describe nuclear phenomena and its correctness. This stage was associated with the observation of the most intense (favored) α-transitions.

The second stage evolved as additional α-spectra and the processes like unfavored or hindered α-transitions were subsequently identified. A description of such transitions became possible after the formulation of the shell model. In this model, α-decay involves two parts: the process of formation (structure part) and the process of penetration through the barrier (energy part). The probability of formation depends on the structure of nuclear states and determines the different classes of α- transitions.

Later the description of the nuclear structure by single particle or collective models constructed on the basis of an infinite oscillator potential constituted the third stage.

1.3 Gamow's theory of α-emission

Since an α-particle is emitted from the nucleus as a discrete particle, one might infer that some tightly bound assembly of two neutrons and two protons pre existed in the nucleus, or a heavy nucleus may have a sub-structure of α-particle.

Although we do not know the exact nature of the forces acting on the α-particle, but it is known that there are repulsive forces due to charges and some strong attractive nuclear short range forces. Due to rapid decline of nuclear forces with distance, a positively charged particle will experience a diminishing attraction near the surface of the nucleus. When receding from the latter and at a certain distance, the forces of attraction will be balanced by coulomb forces of repulsion. From this it follows that the internal part of the nucleus is separated from the outer space by a certain potential barrier, which prevents the emission of the alpha particle from the nucleus.

The figure 1.1 is the plot of potential energy U of an alpha particle as a function of its distance r from the center of a certain heavy nucleus.

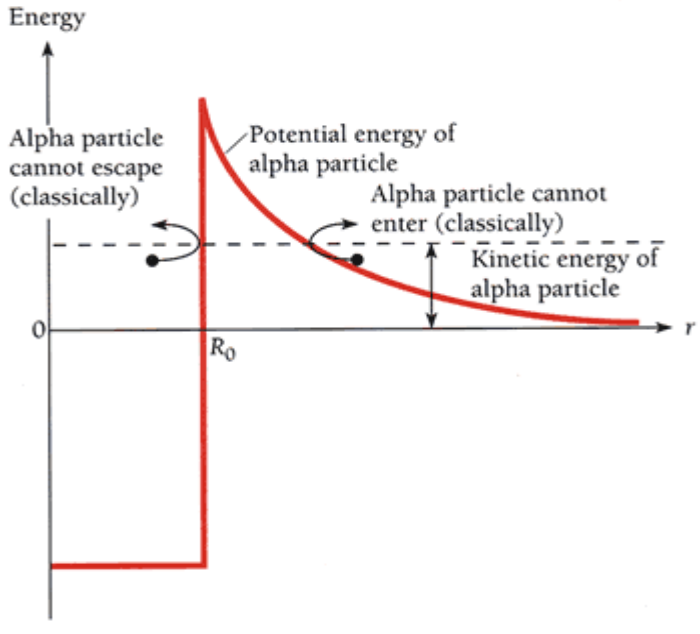

Figure 1.1 α-particle across a potential barrier

The height of this barrier is the potential energy of the alpha particle at r=R. The potential energy V(r) of an alpha particle at a distance r from the centre of the nucleus is given by

$$V(r) = 2(Z - 2)\, e^2 / 4\pi\varepsilon_0 r\,, \qquad r > R \qquad (1.1)$$

In the case of ^{238}U, the height of the potential barrier for alpha particle comes out to be 28 MeV. Thus 28 MeV is the minimum energy that an alpha particle must have, according to classical ideas, in order to escape from the nucleus of ^{238}U. But the energies carried out by α-particles, emitted by radioactive nuclei, are much lower than the heights of the potential barriers of the respective nuclei. Thus it is very interesting to understand how the particles contained inside the nucleus can go over a potential barrier which is more than twice as high as their total energy.

Classical mechanics provided no explanation of this state of affairs, but in 1928, Russian born G. Gamow [2] explained this paradox by means of wave mechanics. If the motion of a particle in the neighbourhood of a potential barrier is treated wave mechanically, it is found that there is finite probability that the particle can leak through the barrier even though its kinetic energy is less than the barrier.

For zero angular momentum problem the wavefunction ψ(r,Θ,ϕ) of the alpha particle with respect to the centre of the daughter nucleus is independent of the angle. The function u(r) = rψ(r) must satisfy the one dimensional wave equation.

$$-\frac{h^2}{2m}\frac{d^2u}{d\,r^2} + [V(r) - E]u = 0 \qquad (1.2)$$

Where m = $M_\alpha M_D/(M_\alpha+M_D)$ is the reduced mass of the α-particle and the daughter nucleus.

E = Kinetic energy of the α-particle

For a rectangular potential barrier of height V and width a

$$V(r) = 0 \qquad r < 0 \text{ and } r > a$$

$$V(r) = V \qquad 0 < r < a \qquad (1.3)$$

As is clear from the figure 1.2 below we have three regions of interest.

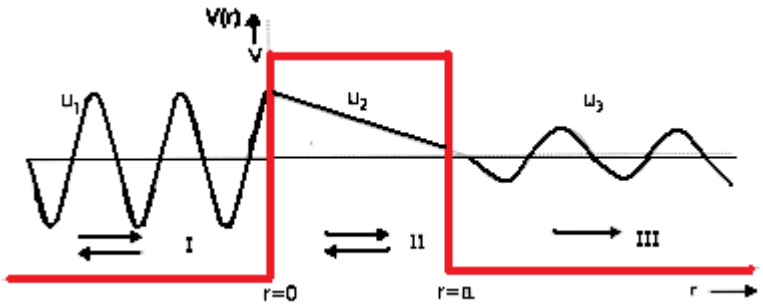

Figure 1.2 Penetration of α-particle across a finite potential barrier [1]

The Schrodinger equation in region 1 and 3 is

$$\frac{d^2u}{dr^2} + \frac{2m}{h^2}Eu = 0 \qquad (1.4)$$

And for region 2, we have

$$\frac{d^2u}{dr^2} + \frac{2m}{h^2}(E - V)u = 0 \qquad (1.5)$$

Since region 1 has both incident and reflected alpha waves , so the solution of the Schrödinger equation is given by

$$u_1 = A_1 e^{ik_1 r} + B_1 e^{-ik_1 r} \qquad (1.6)$$

where

$$k_1 = \sqrt{2mE}/h \qquad (1.7)$$

For region 2, the solution of the Schrodinger equation is given by

$$u_2 = A_2 e^{k_2 r} + B_2 e^{-k_2 r} \quad (1.8)$$

where

$$k_2 = \sqrt{2m(V-E)}/h \quad (1.9)$$

For region 3 the solution of the Schrödinger equation is given by

$$u_3 = A_3 e^{ik_1 r} \quad (1.10)$$

The physical requirement of continuity in the wave functions and their first derivatives with respect to r at the boundaries r = 0 and r = a gives the values of coefficients A_1, A_2, A_3, B_1 and B_2.

The boundary conditions may be written as

at r = 0, $u_1(0) = u_2(0)$; $u_1'(0) = u_2'(0)$

at r = a, $u_2(a) = u_3(a)$; $u_2'(a) = u_3'(a)$ (1.11)

By substituting the values of u_1, u_2 and u_3 in the above boundary conditions we have

$$A_2 = \frac{1}{2} A_3 (1 + ik_1/k_2) e^{(ik_1 - k_2)a} \quad (1.12)$$

$$B_2 = \frac{1}{2} A_3 (1 - ik_1/k_2) e^{(ik_1 + k_2)a} \quad (1.13)$$

and

$$A_1 = \frac{1}{2} A_2 (1 + k_2/ik_1) + \frac{1}{2} B_2 (1 - k_2/ik_1) \quad (1.14)$$

As the velocity of alpha particle in region 1 and region 3 are same, hence the transmission probability of incident particle is given as follows

$$T = \frac{Transmitted\ flux}{Incident\ flux} = \frac{|A_3|^2 \times v}{|A_1|^2 \times v} = \frac{|A_3|^2}{|A_1|^2}$$

Substituting the values of A_1 and A_3, we get

$$T = \left[1 + \frac{V^2}{4E(V-E)}(\sinh k_2 a)^2\right]^{-1} \qquad (1.15)$$

In the limit of thick rectangular barrier, for when $k_2a >> 1$, the transmission coefficient of the alpha particle is approximately expressed as

$$T = \frac{16E(V-E)}{V^2} e^{-2k_2 a} \qquad (1.16)$$

The above equation shows that for a reasonably thick barriers the probability of transmission through the barrier decreases exponentially as the thickness a increases. The dominant term here is the exponential. For the order of magnitude calculation, we may write

$$T = e^{-2k_2 a} \qquad (1.17)$$

This is the Gamow's Formula.

The above equation represents the fraction of the alpha particles that will penetrate the barrier of width a and of height V (> E). If the potential is not constant in the region 0 < r < a, we can always approximate it with a series of small steps, each with a constant potential.

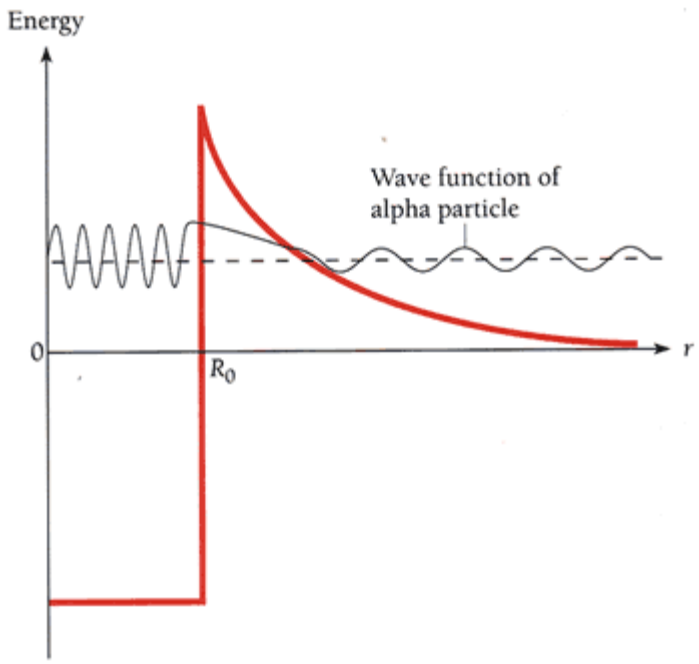

Figure1.3 Mechanism of α-decay

For the α-particles of kinetic energy E, the integral is taken through the whole region between R and r_1, where the coulomb repulsion is greater than the energy of α-particle or the forbidden region of classical mechanics, we have

$$T = e^{-2G} \qquad (1.18)$$

where

$$G = \sqrt{\frac{2m}{h^2}} \int_a^b [V(r) - E]^{1/2} dr \qquad (1.19)$$

is the Gamow factor.

Thus the result of the quantum mechanical calculation for the half- life of α-decay is

$$t_{1/2} = 0.693 \frac{a}{c} \sqrt{\frac{mc^2}{2(V+E)}}\ exp\left\{2\sqrt{\frac{2mc^2}{(hc)^2 E}}\ \frac{zZ'e^2}{4\pi\varepsilon_0}\left(\frac{\pi}{2} - 2\sqrt{\frac{E}{B}}\right)\right\} \qquad (1.20)$$

The agreement between the measured and the calculated α-decay half-lives is not exact, but the calculation is able to reproduce the trend of the half-lives within 1-2 orders of magnitude over a range of more than 20 orders of magnitude.

It is important to note that, we have neglected several important details in the calculation above: we did not consider the initial and the final nuclear states, we did not consider the angular momentum carried by the α-particle, and we assumed the nucleus to be spherical with a mean radius of $1.25A^{1/3}$ fm.

The latter approximation has a very substantial influence on the calculated half-lives. The nuclei with A > 230 have strongly deformed shapes, and the calculated half-lives are extremely sensitive to small changes in the assumed mean radius.

Even though this oversimplified theory is not strictly correct, it gives us a good estimate of the decay half-lives. It also enables us to understand why other decays into light particles are not commonly seen, even though they may be allowed by the Q value. For example, for the decay of ^{220}Th

$$^{220}\text{Th} \rightarrow {}^{12}\text{C} + {}^{208}\text{Po}$$

one gets Q value of 32.1 MeV and subsequently one may get $t_{1/2} = 2.3 \times 10^6$ sec for the ^{220}Th decay into ^{12}C. This is a factor of 10^{13} longer than the α-decay half-life and thus the decay will not easily be observable.

The theory as presented above applies only to ground state decays between even-even nuclei, where α- particles have no internal angular momenta. These ground state α-transitions are known as the favored α-transitions. In addition to the favored α-transition, the ground state of the parent nuclei can also decay to the excited states of the daughter nuclei i.e. to the members of ground state rotational band. These α-transition belong to the unfavored cases, which are strongly hindered as compared with the ground state ones and the angular momentum carried away by the α-particle is not equal to zero.

1.4 Angular momentum in α-decay

Up to this point we have neglected the discussion on angular momentum carried by the α-particle. In a transition from an initial nuclear state of angular momentum I_i to the final state I_f, the angular momentum of α particle can range between $I_i + I_f$ and $| I_i - I_f |$. The nucleus ^{4}He consists of two protons and two neutrons, all in 1s states and all with their spins coupled pairwise to 0. The spin of the α-particle is therefore zero, and the total angular momentum carried by α-particle in a decay process is purely orbital in character. Let us designate it as ℓ_α.

We must recognize that we have neglected one very significant feature of α-decay that is a given intial state can populate many different final states in the daughter nucleus. This property sometimes known as the “fine structure” of α-decay, but of course has nothing whatever to do with atomic fine structure. The figure 1.4 shows the α-decay ^{242}Cm to the excited states of ^{238}Pu. The initial state is spin zero, and thus the angular momentum carried away by the α-particle ℓ_α is equal to the angular momentum of the final nuclear state I_f. As can be seen from the figure the α-decay to the different states of ^{238}Pu has different intensities.

The intensity depends on the wavefunctions of the initial and the final states and also on the angular momentum, ℓ_α. The centrifugal potential term, $\ell(\ell + 1)\hbar^2/2mr^2$ that is included in the spherical coordinates is always positive and has the effect of raising the potential energy, thus increasing the thickness of the barrier that α-particle must penetrate. As the barrier thickness increases for excited states (i.e. $\ell_\alpha = 2^+, 4^+, \ldots$) the decay intensity also decreases and such decays are termed as unfavored or hindered α-transitions.

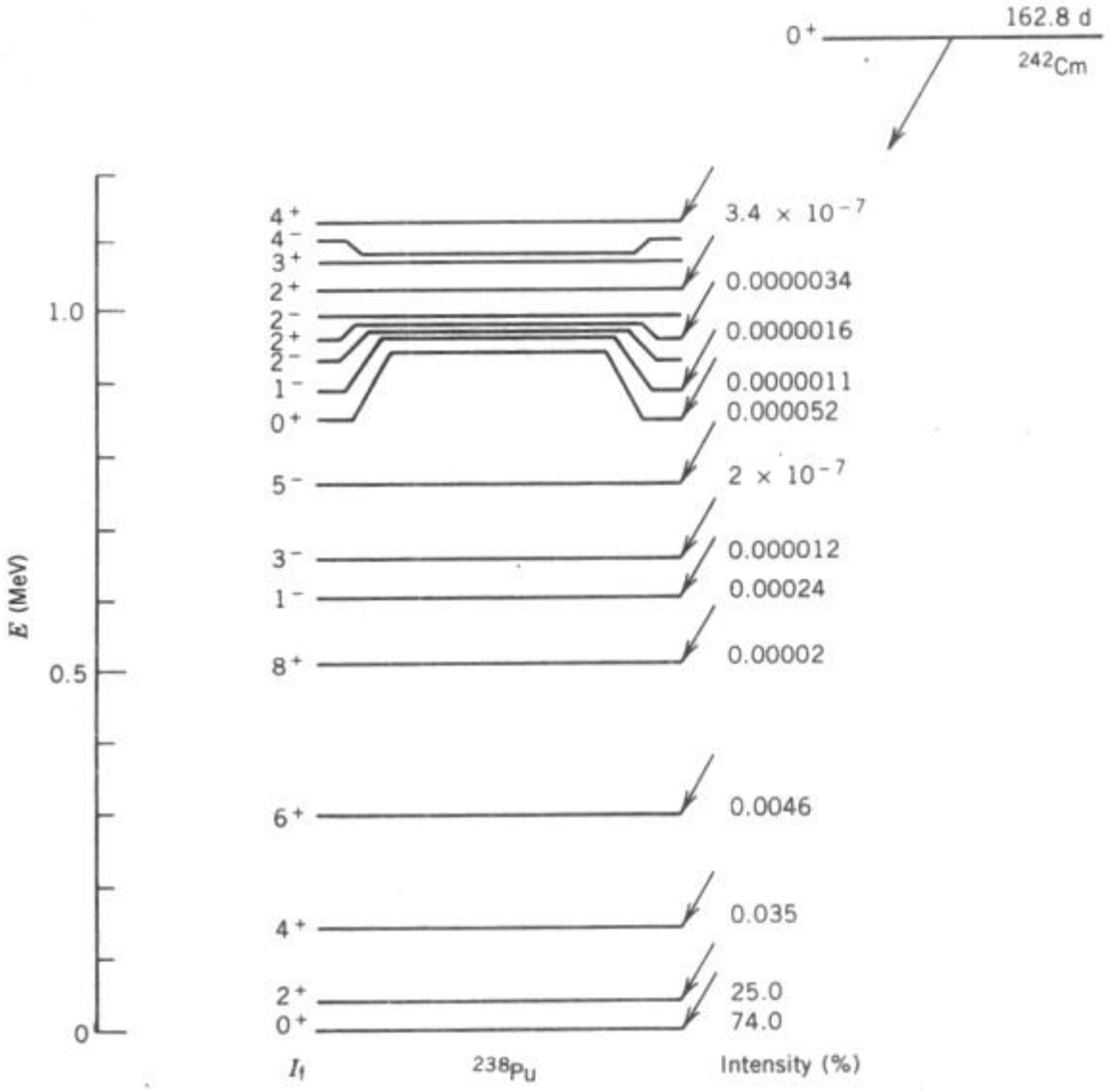

Figure 1.4 Decay of ^{242}Cm to the excited states of ^{238}Pu [1]

1.5 Energetics of α-decay

The energy released in α-decay, Q, is determined by the difference in mass of the parent nucleus and decay products, which include the daughter nucleus and the α-particle. For example, consider the decay of ^{232}Th (Z=90) into ^{228}Ra (Z=88) plus an α-particle. This can be written as

$$^{232}\text{Th} \rightarrow {}^{228}\text{Ra} + \alpha \quad (= {}^{228}\text{Ra} + {}^{4}\text{He})$$

The energy Q is measured in terms of atomic masses. If M_p is the mass of parent nucleus, M_D that of daughter nucleus and M_{He} that of helium nucleus, then the decay energy Q is given by conservation of mass energy as

$$\frac{Q}{c^2} = M_p - (M_D + M_{He}) \qquad (1.21)$$

The kinetic energy of the α-particle (for decays to the ground state of daughter nucleus) is slightly less than the decay energy Q because of the small recoil energy of the daughter nucleus.

If parent nucleus is at rest when it decays, the daughter nucleus and α-particle must have equal and opposite momenta. If p is the magnitude of the momenta of either particle then decay energy is

$$Q = \frac{p^2}{2M_D} + \frac{p^2}{M_{He}} = \frac{p^2}{2M_{He}}\left(1 + \frac{M_{He}}{M_D}\right) \qquad (1.22)$$

Then, writing E_α for $p^2/2M_{He}$ and $M_{He}/M_D = 4/(A - 4)$, where A is the mass of parent nucleus, we have

$$E_\alpha = \frac{A-4}{A} Q \qquad (1.23)$$

Since A is much greater than 4 for most nuclides that decay by α-decay, E_α is nearly equal to Q. For the ^{232}Th decay discussed above, the α-particle carries away about 98 percent of the decay energy Q. If all the α-decays proceeded from the ground state of the parent nuclei to the ground state of the daughter nucleus, the emitted α-particles would all have the same energy related to the total energy available, Q. When the energies of emitted α-particles are measured with high resolution a spectrum of energies is observed as is shown for the decay of ^{227}Th into ^{223}Ra in fig.1.5.

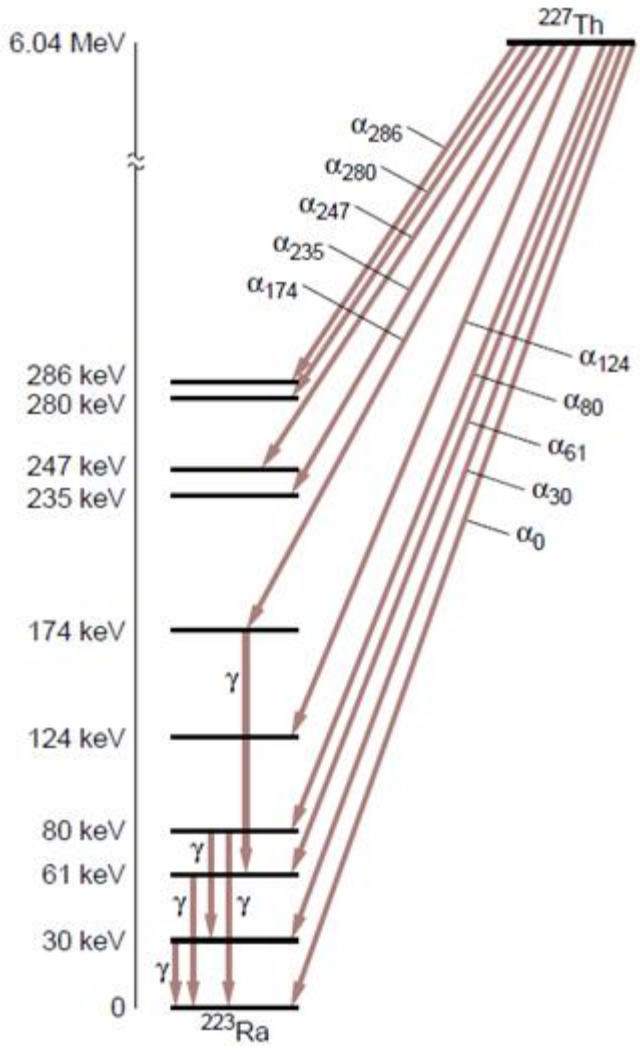

Figure 1.5 Decay of ^{227}Th to the excited states of ^{223}Ra

1.6 α-Decay Spectroscopy

Now the question arises, What can we learn about the energy levels of nuclei by studying the α decay?

Let's consider, for example, the decay of ^{227}Th to the various energy levels of ^{223}Ra. The figure 1.5 shows the energy spectrum of α-decays from the decay of ^{227}Th. As can be clearly seen there are 10 distinct groups of α-particles, each group

presumably represents the decay to a different excited state of ^{223}Ra. How can one use this information to construct the level scheme of ^{223}Ra?

Based on the α-spectrum, one can find the energy and intensity of each α group. The energy is found by comparing with decays of known energy and intensity is calculated from the area of each peak.

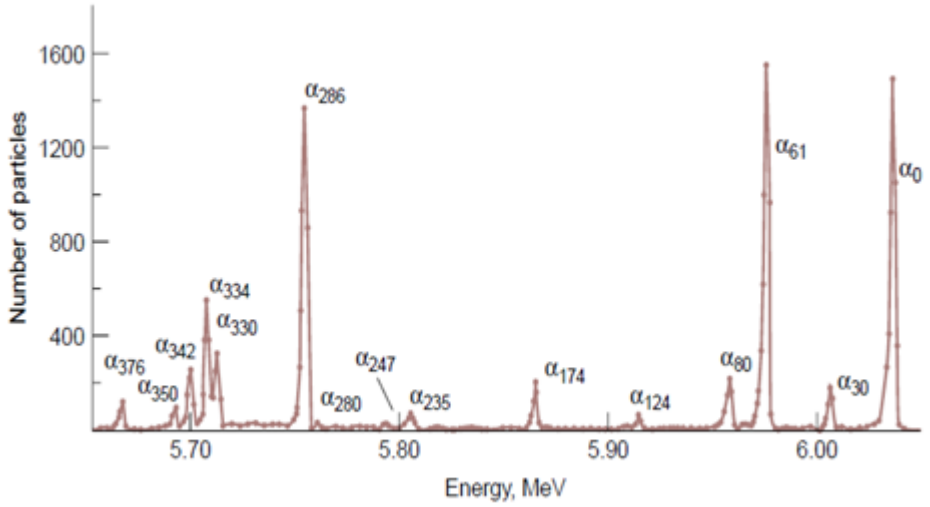

Figure 1.6 Alpha particle spectrum from ^{227}Th.

The different ^{223}Ra excited states will quickly decay to the ground state by emitting γ-ray photon, so in constructing the decay scheme it is helpful to have the energies and intensities of the γ rays as well.

Let's assume that, the highest energy α-decay populates the ground state of ^{223}Ra (In an even-even nucleus, this would be very good assumption, because 0^+—0^+ α-decays are very strong and not inhibited by any differences between the wave functions of the initial and final ground states. In odd-A nucleus, the initial and final ground states may have very different characters so that the decay to the ground state may be very weak or even vanishing.) The decay just lower in energy differs from ground state decay by about 30 KeV. Assuming this to populate the first excited state, one can find among the γ-transition one of energy as 30 KeV, which presumably represents the transition between the first excited state and the ground state.

The interpretation of the remaining states can be aided by α-γ coincidence studies, in which only those γ transition are selected that follow a given α-decay within a certain short time interval. All these states form the ground-state rotational band whose angular momentum have values I = 0^+, 2^+, 4^+,…. (Because the ground state of an even-even nucleus is always 0^+ state, and the mirror symmetry of the nucleus restricts the sequence of rotational states in this special case to even values of I)

Theoretically, the hindered α-transitions are an effective tool for the study of the properties of α-emitters especially in the neighbourhood of shell closures because it is closely related to the internal structure of the nuclei. The study of α-decay has received particular attention in the search of new elements because the observed decay mode of newly synthesized SHN is mainly α-decay.

The concept of unfavored hindered alpha transition is yet to be explored completely and preliminary investigation reveal that the α-decay occurring between the ground state of parent nucleus to the excited states of daughter nucleus can perhaps give useful inputs to extract information regarding nuclear deformations in the unexplored heavy / superheavy mass region.

REFERENCES

[1] Introductory Nuclear Physics, author Kennenth S. Krane

[2] G.Gamow, Z. Phys. **51**, 204 (1928)

[3] E.U.Condon and R.W.Gurney, Nature (London) **122**, 439 (1928)

Chapter 2

Methodology

2.1 Introduction

A comprehensive study of various types of emission from the ground state as well as excited states of heavy and super heavy nucleus (SHN) formed in low energy reaction is important, as it gives information about the nuclear structure aside the underlying nuclear forces. At low energies an average nuclear force field acts between decaying fragments which in turns ensure possibility of more than one decay path. This average nuclear force field is largely influenced by entrance channel, angular momentum and the temperature consideration along with contribution of deformation and orientation effects. An extensive study of these nuclear properties lead to a better understanding of reaction dynamics of rare nuclear species that make the unexplored part of the nuclear chart, called exotic nuclei.

The main aim of the work is to study heavy ion reaction dynamics especially the decay of heavy nuclei using the dynamical cluster decay model (DCM) [1-9] .It is important to note that deformation and orientation effects of the reaction partner and decay products are explicitly included along with temperature and angular momentum contribution in this model.

This model is a two step model, where the first step is quantum mechanical preformation probability P_0 of the decay products or cluster formed in the mother nuclei and the second step is the penetration of the fragments/clusters through the interaction barrier. The Penetration probability P is given in section 2.8. These two crucial parameters (P_0 and P) have been developed and used [1], [11-13], to calculate the α-decay branching ratios to the excited states of even-even nuclei. The assault frequency, υ_0 with which the preformed cluster tries to tunnel the barrier in the ground state decay is discussed in section 2.6.

2.2 The Dynamical Cluster Decay Model (DCM) For Hot and Rotating Compound Nucleus

The dynamical cluster decay model (DCM) [1-9] for hot and rotating nuclei (i.e. angular momentum and temperature both not equal to zero) is a reformation of the preformed cluster model of Gupta and collaborators for ground state decay (ℓ =0,t=0)in cluster radioactive (CR)and related phenomena [14-16], [11] .Like PCM, DCM is also based upon the dynamical (or quantum mechanical) fragmentation theory of cold phenomena in heavy ion reaction and fission dynamics .In DCM, besides the temperature and angular momentum effects in the decay of excited compound nuclei ,the deformation and orientation effect of the decay products are also taken care, especially in the decay of heavy excited CN for which the deformation of the decay product seems to play significant role. The DCM, worked out in terms of the collective coordinates of mass asymmetry $\eta=\frac{A_{1-}A_2}{A_{1+}A_2}$ and relative separation R respectively gives

(i). The nucleon-division (or exchange)between the outgoing fragments ,and

(ii). The transfer of kinetic energy of incident channel (E_{cm}) to internal excitation (total excitation or total kinetic energy ,TXE or TKE) of the outgoing channel. It may be noted that the fixed decay point R = R_a (defined later), at which the process is calculated depends upon temperature T as well as on η (i.e.R(T, η)). This energy transfer process can be calculated as follows with the help of Fig 2.1

$$\mathrm{E}^*_{\mathrm{CN}} = E_{cm} + Q_{in} = |Q_{out}| + TKE(T) + TXE(T) \qquad (2.1)$$

The CN excitation $\mathrm{E}^*_{\mathrm{CN}}$ is related to temperature T (in MeV) and is given by

$$\mathrm{E}^*_{\mathrm{CN}} = \frac{1}{9}AT^2 - T(Mev) \qquad (2.2)$$

.

Using the decoupled approximation to R and η–motions, the DCM define the decay cross section, in terms of partial waves, as [3]-[9];

$$k = \sqrt{\frac{(2\mu Ec.m)}{h^2}}; \sigma = \sum_{l=0}^{lc} \sigma l = \frac{\pi}{k^2} \sum_{l=0}^{lc} (2l+1) PoP \qquad (2.3)$$

Where P_0 ,the preformation probability refers to η-motion and P, the penetrability to the R- motion. Here the complex fragments (both light and heavy fragments) are treated as the dynamical collective mass motion of preformed cluster or fragments through the barrier .The structure information of the CN enters the model via preformation probability P_0 (also known as spectroscopic factor)of the fragments given by the solution of stationary Schrödinger equation in η at the fixed R=R_a ,the first turning point of the penetrability path shown in figure 2.1for the different ℓ -values .

$$\left\{ -\frac{\hbar^2}{2\sqrt{B_{\eta\eta}}} \frac{\partial}{\partial \eta} \frac{1}{\sqrt{B_{\eta\eta}}} \frac{\partial}{\partial \eta} + V_R(\eta, T) \right\} \psi^{\nu}(\eta) = E^{\nu} \psi^{\nu}(\eta) \qquad (2.4)$$

with ν =0,1,2,3,….referring to the ground state and excited state solution .

For the decay of the hot compound nucleus, we use the postulate of first turning point

$$R_a = R_t + \Delta R(T) \qquad (2.5)$$

Where

$$R_t = R_1 + R_2 \qquad (2.6)$$

∆R(T) is the neck length parameter that assimilates the neck formation effects .This method is introducing a neck length parameter similar to that used in scission point [17] and saddle point [18],[19] statistical fission model. The R_i are radius vectors which are also made temperature dependent can be calculated as

$$R_i(\alpha_i) = R_{0i}\left[1 + \sum_{\lambda} \beta_{\lambda i} Y_{\lambda}^{(0)}(\alpha_i)\right] \qquad (2.7)$$

with

$$R_{0i}(T) = 1.28A_i^{1/3} - 0.76 + 0.8A_i^{-1/3} \times (1 + 0.0007T^2) \qquad (2.8)$$

The corresponding potential V (R_a) acts like an effective Q-value, Q_{eff} , for the decay of the hot CN at temperature T, to two exit-channel fragments observed ing.s. (T=0), defined by

$$Q_{eff}(T) = B(T) - [B_L(T=0) + B_H(T=0)]$$
$$= TKE(T) = V\big(R_a(T)\big) \qquad (2.9)$$

with B's as the respective binding energies.

The above defined decay of a hot CN into two cold (T=0) fragments, via Eq.(2.8), could apparently be achieved only by emitting some light particle (s)(LPs), like n, p, α, or γ-rays of energy

By defining Q_{eff} (T) as in Eq. (2.8), in this model we treat the LP emission at par with the heavy fragments, called intermediate mass fragments (IMFs) emission. Thus, in this model a non-statistical dynamical treatment is attempted for not only the emission of IMFs but also of multiple LPs, understood so-far only as the statistically evaporated particles in a CN emission. It may be reminded here that the statistical model (CN emission) interpretation of IMFs is not as good as it is for the LP production [17], [18].

In terms of Q_{eff} (T), the second turning R_b satisfies (see Fig. 2.1)

$$V(R_a,\ l) = V(R_b,\ l) = Q_{eff}(T,\ l) = TKE(T) \qquad (2.10)$$

with the l -dependence of R_a defined by

$$V(R_a, l) = Q_{eff}(T,\ l = 0) \qquad (2.11)$$

which means that the R_a, given by Eq. (2.4), is the same for all l -values, and that V (R_a, l) acts like an effective Q-value, Q_{eff} (T, l), given by the total kinetic energy TKE(T). Then, using (2.9), $R_b(l)$ is given by the l -dependent scattering potentials, at fixed T as

$$V(R,T,l) = V_c(Z_i,\beta_{\lambda i},\theta_i,T) + V_p(A_i,\beta_{\lambda i},\theta_i,T) + V_l(R,A_i,\beta_{\lambda i},\theta_i,T) \qquad (2.12)$$

which is normalized to the exit channel binding energy B_L(T) + B_H(T). Such a

potential is illustrated in Fig 2.1 $^{246}Cf \rightarrow {}^{242}Cm + {}^{4}He$, at ℓ =0 value. The second turning point R_b is marked for the ℓ = 0ħ case of $R_a = R_t + \Delta R(T)$. The decay path for the l -values begins at $R = R_a$.

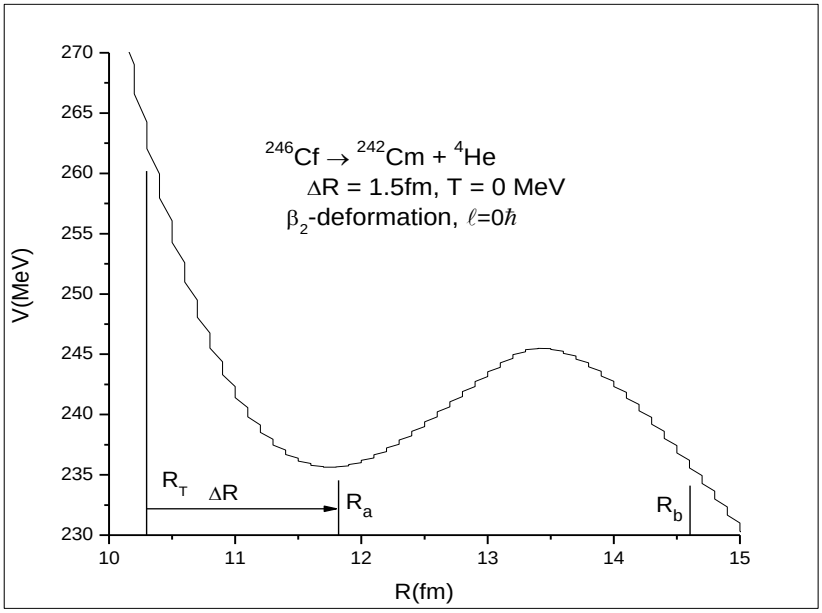

Fig.2.1. Scattering Plot for $^{246}Cf \rightarrow {}^{242}Cm + {}^{4}He$ reaction

The collective fragmentation potential V(R,η,T) in Eq. (2.12) is calculated according to the Strutinsky method by using the T-dependent liquid drop model energy V_{LDM} of [26]. The "empirical" shell corrections δU are of Ref. [27] (In the Appendix of [3] and Eq. (8) of [4], a_a=0.5, instead of unity). Then, including the T-dependence also in Coulomb, nuclear proximity, and l -dependent potential in complete sticking limit of moment of inertia, we get

$$V(R,\eta,T) = \sum_{i=1}^{2}[V_{LDM}(A_i, Z_i, T) + \sum_{i=1}^{2}[\delta Ui]exp\left(\frac{-T^2}{T_0^2}\right) + V_c(Z_i, \beta_{\lambda i}, \theta_i, T) + V_P(A_i, \beta_{\lambda i}, \theta_i, T) + V_l(R, \beta_{\lambda i}, \theta_i, T) \quad (2.13)$$

2.3 The Proximity Potential

When two surfaces approach each other within a small distance of less than ~ 2fm, comparable with the surface thickness of interacting nuclei, or when a nucleus is at the verge of dividing into two fragments, then the two surfaces actually face each other across a small gap or crevice. In both cases, the surface energy term alone could not give rise to the strong attraction that is observed when the two surfaces are brought in close proximity. Such additional attractive forces are called proximity forces and the additional potential due to these forces is called the nuclear proximity potential.

Blocki et al. [20] have reanalyzed and extended a theorem, originally due to Deryagin [21], according to which the force between two gently curved surfaces in close proximity is proportional to the interaction potential per unit area between the two flat surfaces. The original expression of Blocki based on the pocket formula was for spherical nuclei, and is given as

$$V_p(S_0) = 4\pi\bar{R}\gamma b\Phi(S_0) \qquad (2.14)$$

Φ (s_0) is the universal function, independent of the shapes of nuclei or the geometry of nuclear system, but depends on the minimum separation distance

$$\Phi(s_0) = \begin{cases} -1/2(s_0 - 2.54)^2 - (s_0 - 2.54)^3 \\ -3.437\exp(-s_0/0.75) \end{cases}$$

respectively, for $s_0 \leq 1.2511$ and $s_0 \geq 1.2511$. Here, s_0 is defined in units of b, i.e. s_0 is s_0/b. This function is defined for negative (the overlap region), zero (touching configuration) and positive values of s_0. For a fixed R, the minimum distance s_0 for spherical nuclei is defined as

$$S_0 = R - R_1 - R_2 \qquad (2.15)$$

where $R = 1.07A_i^{1/3}$(i=1,2). b is the diffuseness of the nuclear surface given by

$$b = \left[\frac{\pi}{2}\sqrt{3}\ln 9\right]_{t_{10-90}} \qquad (2.16)$$

where $t_{10\text{-}90}$ is the thickness of the surface in which the density profile changes from 90% to 10%. The value of b ~1 fm. The γ is the specific nuclear surface tension given by

$$\gamma = 0.9517\left[1 - 1.7826\left(N - \frac{Z}{A}\right)^2\right] MeV\ fm^{-2} \qquad (2.17)$$

R' is the mean curvature radius of the reaction partners, characterizing the gap,which for spherical nuclei is given by

$$\bar{R} = \frac{R_1 R_2}{R_1 + R_2} \qquad (2.18)$$

2.4 The Coulomb potential

Coulomb potential describes the force of repulsion between two interacting nuclei due to their charges. It acts along the line joining the two nuclei. The Coulomb potential for two interacting spherical nuclei is given as

$$V_c = \frac{Z_1 Z_2 e^2}{R} \qquad (2.19)$$

For interacting deformed and oriented nuclei, different authors [22], [24] have derived it differently. In this thesis work, we have started with Coulomb potential of Wong [23], given for two non-overlapping charge distributions, having quadrupole deformations only, i.e.,

$$V_c = \frac{Z_1 Z_2 e^2}{R} + \sqrt{\frac{9}{20\pi}}\left(\frac{Z_1 Z_2 e^2}{R^3}\right)\sum_{i=1}^{2} R_i^2(\alpha_i)\beta_{2i}P_2(\cos\theta_i) + \left(\frac{3}{7\pi}\right)\left(\frac{Z_1 Z_2 e^2}{R^3}\right)\sum_{i=1}^{2} R_i^2[\beta_{2i}P_2(\cos\theta_i)]^2 \qquad (2.20)$$

In this expression, the quadrupole-quadrupole interaction term, proportional to $\beta_{21}\beta_{22}$, is neglected since it has a short-range character.

2.5 Rotational Energy due to angular momentum

In the case of unfavored α-decays such as ground state of the parent nucleus to the ground and excited states of the daughter nucleus the angular momentum carried away by the α-particle is not 0. Thus rotational energy due to angular momentum has been introduced as

$$V_l = \frac{h^2 l(l+1)}{8\pi^2 I} \qquad (2.21)$$

with I = μR^2, is the non-sticking limit of moment of inertia with as the $\mu = \frac{A1A2}{A1+A2} m$ reduced mass. m is the nucleon mass. In the complete sticking limit, the moment of inertia I is given as,

$$I = \mu R^2 + \frac{2}{5} A_1 m R_1^2 + \frac{2}{5} A_2 m R_2^2 \qquad (2.22)$$

However, for the relative separation of interest here, we use the sticking limit. It is relevant to mention here that value of angular momentum extracted experimentally, is based upon moment of inertia limit.

2.6 Assault Frequency, υ_0

For the cluster decay studies in the following section, another quantity of interest is the assault frequency υ_0 defined as,E_2

$$\upsilon_0 = \frac{v}{R_0} = \frac{1}{R_0}\sqrt{\frac{2E_2}{\mu}} \qquad (2.23)$$

where R_o is the radius of parent nucleus and $E_2 = 1/2\mu v^2$ is the kinetic energy of the emitted cluster. Since both the emitted cluster and the daughter nucleus are produced in the ground state, the entire positive Q-value is the total kinetic energy ($Q = E_1 + E_2$) available for the decay process, which is shared between two fragments, such that for the emitted cluster

$$E_2 = \left(\frac{A_1}{A}\right) Q \qquad (2.24)$$

and, $E_1 = Q - E_2$ is the recoil energy of the daughter nucleus.

2.7 Solution of the Schrödinger Equation and the fragments Preformation Probability P_0

Once the Hamiltonian

$$\mathrm{H} = -\frac{\hbar^2}{2\sqrt{\mathrm{B}_{\eta\eta}}}\frac{\partial}{\partial\eta}\frac{1}{\sqrt{\mathrm{B}_{\eta\eta}}}\frac{\partial}{\partial\eta} - \frac{\hbar^2}{2\sqrt{\mathrm{B}_{\mathrm{RR}}}}\frac{\partial}{\partial\mathrm{R}}\frac{1}{\sqrt{\mathrm{B}_{\mathrm{RR}}}}\frac{\partial}{\partial\mathrm{R}} + \mathrm{V}(\eta) + \mathrm{V}(\mathrm{R}) \qquad (2.25)$$

is established, the Schrödinger equation in mass fragmentation co-ordinate η

$$\left[-\frac{\hbar^2}{2\sqrt{B_{\eta\eta}}}\frac{\partial}{\partial\eta}\frac{1}{\sqrt{B_{\eta\eta}}}\frac{\partial}{\partial\eta} + V(\eta)\right]\psi^{v}(\eta) = E_{\eta}^{v}\psi^{v}(\eta) \qquad (2.26)$$

can be solved. On solving the above equation numerically, $|\psi^{v}(\eta)|^2$ gives the probability P_0 of finding the mass fragmentation η at a fixed R on the decay path.

$$P_0(A_2) = |\psi^{v}(A_2)|^2 \qquad (2.27)$$

For fission studies, like the spontaneous fission and fission through the barrier, the motion in R at the saddle point is adiabatically slow as compared to the η motion. Therefore, the potential is minimized in the neck and deformation coordinates $ß_1$ and $ß_2$ at each R and η values. Starting from the nuclear ground state in spontaneous fission or cluster decay, and to have complete adiabaticity, only the lowest vibrational state $v = 0$ is occupied. Then, the mass (or charge) distribution yield, proportional to the probability $|\psi^{(0)}(\eta)|^2$ or $|\psi^{(0)}(\eta_z)|^2$ of finding a certain

mass (or charge) fragmentation η (or η Z) at a position R on the decay path, when scaled to, say, mass A_2 of one of the fragments (d η =2/A) is given by:

$$Y(A_2) = \left|\psi_R^{(0)}(A_2)\right|^2 \frac{2}{A}\sqrt{B_{\eta\eta}(A_2)} \qquad (2.28)$$

However, if the system is excited or we allow interaction between various degrees of freedom, higher values of v would also contribute. These enter via the excitation of higher vibrational states, and through the temperature dependent potential V and masses Bij The effect of adding temperature on potential V and masses Bij is to reduce the shell effects in them, resulting finally in the liquid drop potential VLDM and smoothed (averaged) masses Bij for the systems to be very hot. Apparently, cold fission means taking both the potential V and masses Bij with full shell effects included in them and hot fission means using the VLDM and smoothed (averaged) masses Bij. The possible consequence of such excitations are included here by assuming a Boltzmann like occupation of excited states

$$|\psi(\eta)|^2 = \sum_{v=0}^{\infty} |\psi^v(\eta)|^2 \, exp\left(-\frac{E_\eta^v}{T}\right) \qquad (2.29)$$

Note that we are dealing here with a directly measurable quantity, the mass (or charge) asymmetry, which works dynamically as mass (or charge) transfer coordinate. Thus, the calculated yields Y (A_i) (or Y (Z_i)) are directly comparable with experiments. It may be stressed that there is no free parameter in these calculations. The nuclear shape, once minimized in the neck and deformation coordinates ß$_1$ and ß$_2$ at a given R (=R_{saddle}), remains fixed for both the mass and charge distributions of fission or decay fragments.

2.8 Penetrability, P

The penetrability P measures the capability of the fragments nucleus to penetrate the potential barrier generalized during the compound nucleus formation and is calculated using WKB approximation.

The WKB integral between R_a and R_b is .

$$P = exp\left[-\frac{2}{\hbar}\int_{R_a}^{R_b}\{2\mu[V(R) - Q_{eff}]\}^{1/2}dr\right] \qquad (2.30)$$

with R_b as the second turning point , satisfying

$$V(R_a, l) = V(R_b, l) = Q_{eff}(T, l=l_{min}) = TKE(T),$$

which means that the potential $V(R_a, l)$, corresponmd to R_a ,acts like an effective Q-value, Q_{eff} (T, l=l_{min}),in the WKB integral, and gives the total kinetic energy TKE(T), where l_{min}=0 or refers to the minimum l-value that starts to contribute to WKB integral.

The daughter nucleus after the disintegration has the most probability of staying in its ground state and probability of its staying in the excited state is much smaller. Therefore it is assumed that the probability of the daughter nucleus to stay in the excited states ($I^+ = 0^+, 2^+, 4^+,\ldots\ldots$) obeys the Boltzmann distribution [25]

$$\omega_l(E_l^*) = exp(-cE_l^*) \qquad (2.30)$$

E_l^* is the excitation energy of the I^+ state and c is the free parameter. The value of c in the above excitation probability function is taken as 25 in the framework of DCM. It is important to recall that the rotational energy term (carrying the effect of angular momentum) is always positive and hence raises the potential energy barrier height. As a result the decay to the excited states of daughter nuclei are in general unfavored or hindered.

The probability of α-transition from the ground state of the parent nucleus to the excited states of the daughter nucleus is given as [25]

$$I_{l^+} = \omega_l(E_l^*)P(l, E_l^*)P_0(l, E_l^*) \qquad (2.31)$$

Two approaches has been used to calculate the α-decay branching ratios to the ground and excited states of even-even nuclei.

The first is the Unified Fission approach where the preformation probability P_0 is assumed to be 1, that is in this model it is assumed that α particle exists as an entity within the heavy nucleus.

And the second is Preformed Cluster approach under which the preformation probability is calculated by solving the Schrodinger equation as discussed in section 2.7, where it is assumed that the fragment is having some definite probability of formation before it decays from CN state.

With the help of transition probability I_{l^+} the branching ratio to each state of the rotational band of the daughter nucleus can be calculated as [25]

$$b_{g.s.}^{0^+}\% = (I_{0^+}/I_{0^+} + I_{2^+} + I_{4^+} + I_{6^+} + \ldots\ldots) \times 100\%$$

$$b_{g.s.}^{2^+}\% = (I_{2^+}/I_{0^+} + I_{2^+} + I_{4^+} + I_{6^+} + \ldots\ldots) \times 100\%$$

$$b_{g.s.}^{4^+}\% = (I_{4^+}/I_{0^+} + I_{2^+} + I_{4^+} + I_{6^+} + \ldots\ldots) \times 100\%$$

and so on.

It will be interesting to see the decay probability of stable parent into the excited states of the daughter using Unified fission and Preformed cluster approach within the framework of DCM.

REFERENCES

[1] R.K. Gupta, M. Balasubraniam, C. Mazzocchi, M. La Commara, and W. Scheid, Phys. Rev. C **65**, 024601 (2002).

[2] M.K. Sharma, R.K. Gupta, and W. Scheid, J. Phys. G **26**, L45 (2000).

[3] R.K. Gupta, R. Kumar, N.K. Dhiman, M. Balasubraniam, W. Scheid, and C. Beck, Phys. Rev. C **68**, 014610 (2003).

[4] M. Balasubraniam, R. Kumar, R.K. Gupta, C. Beck, and W. Scheid, J. Phys. G **29**, 2703 (2003).

[5] R.K. Gupta, M. Balasubraniam, R. Kumar, D. Singh, and C. Beck, Nucl. Phys. A **738**, 479c (2004).

[6] R.K. Gupta, M. Balasubramaniam, R. Kumar, D. Singh, C. Beck, and W. Greiner, Phys. Rev. C **71**, 014601 (2005).

[7] B.B. Singh, M.K. Sharma, R.K. Gupta, and W.Greiner,Int.J. Mod.Phys.E15, 699 (2006)

[8] R.K. Gupta, M. Balasubraniam, R.Kumar, D.Singh ,S.K. Arun and W.Greiner,J.Phys .G:Nucl.Part. Phys. **32**, 345(2006)

[9] B.B. Singh, M.K. Sharma, R.K. Gupta,Phys.Rev. C **77**, 054613 (2008)

[10] J. Maruhn and W. Greiner, Phys. Rev. Lett. **32**, 548 (1974).

[11] B.B. Singh, S.K. Arun, M.K. Sharma , S. Kanwar and Raj K. Gupta ,DAE Nucl.Phys.(Roorkee), Accepted(2008)

[12] R.K. Gupta, N.Singh, and M. Manhas, Phys. Rev. C **70**, 034608 (2004)

[13] R.K. Gupta ,M.balasubramaniam, R.Kumar, N.Singh, M.Manhas, and W. Greiner, J.Phjs. G: Nucl.Part. Phys. C **31**, 631(2005).

[14] S.S. Malik and R.K.Gupta, Phys.Rev.C **39**, 1992(1989)

[15] S. Kumar and R.K.Gupta, Phys.Rev. C **49**, 1922(1994).

[16] S. Kumar and R.K.Gupta, Phys. Rev. C **55**, 218 (1997).

[17] T. Matsuse, C. Beck, R. Nouicer, and D. Mahboub, Phys. Rev. C **55**, 1380 (1997).

[18] S.J. Sanders, Phys. Rev. C **44**, 2676 (1991).

[19] S.J. Sanders, D.G. Kovar, B.B. Back, C. Beck, D.J. Henderson, R.V.F. Janssens, T.F. Wang, and B.D. Wilkins, Phys. Rev. C **40**, 2091 (1989t).

[20] J. Blocki, J. Randrup, W. J. Swiatecki, and C. F. Tsang, Ann. Phys. (NY) **105**, 427 (1977).

[21] Deryagin, Kolloid Z. 69, 155 (1934).

[22] N. Malhotra and R.K. Gupta, Phys. Rev. C **31**, 1179 (1985).

[23] C Y Wong, Phys. Rev. Lett. **31**, 766 (1973).

[24] R Aroumougame and R K Gupta, J. Phys. G: 6, L155 (1980).

[25] Y.Z.Wang, H.F.Zhang, J.M.Dong, G.Royer, Phys. Rev. C **79**, 014316 (2009)

[26] N.J. Davidson, S.S. Hsiao, J. Markram, H.G. Miller, and Y. Tzeng, Nucl.

Phys. A 570, 61c (1994).

[27] W. Myers and W.J. Swiatecki, Nucl. Phys. 81, 1 (1966).

Chapter 3

Results and discussions

The *α*-decay process was first explained in 1928 by Gamow [1] and by Condon and Gurney [2] as a quantum tunneling effect. It is perhaps the first example which emphasized on the use of quantum mechanics to describe nuclear phenomena and related concepts. On the basis of Gamow's theory, the experimental *α*-decay half-lives of nuclei can be well explained by both phenomenological and microscopic models. Such *α*-decay calculations are mainly concentrated on the favored cases, e.g., the ground state *α* transitions of even-even nuclei ($\Delta l = 0$). In addition to the favored *α*-transitions, the ground state of the parent nucleus can also decay to the excited states of the daughter nucleus ($\Delta l \neq 0$). Recently, there is increasing interest in two kinds of *α*-transitions of even-even nuclei from both experimental and theoretical sides, i.e., the *α*-decay to excited states and to members of the ground state rotational bands. These *α*-transitions belong to the unfavored cases, which are strongly hindered as compared with the ground state ones. Theoretically, the hindered *α*-transition is an effective tool for the study of the properties of *α*-emitters because it is closely related to the internal structure of nuclei. However, it is difficult to describe quantitatively the unfavored *α*-transitions because of the influence of both the nonzero angular momentum and the excitation of nucleons, especially for *α*-emitters in the neighborhood of shell closures. Although the favored *α*-decay model can be straightforwardly applied to the unfavored *α*-transition, the calculated branching ratios usually deviate significantly from the experimental data. Thus it is necessary to improve the favored *α*-decay model to describe the unfavored hindered *α*-decay. The theoretical predictions on unfavored hindered *α*-transitions are extremely useful for future studies and investigations planned by experimental groups.

In recent work [3] the model was improved by taking into account the influence of the angular momentum of the *α*-particle and the excitation probability of the

daughter nucleus, investigating the hindered *α*-transitions of even-even nuclei with mass numbers 180 < A < 202 and A > 224.

Here the Generalized Liquid Drop Model (GLDM) was used [3] to calculate the α-decay branching ratios to the rotational band of the daughter nuclei in the decay of ^{238}Pu, ^{242}Cm and ^{246}Cf nuclei. As a possible extension of this work we intend to apply Dynamical Cluster Decay Model where the fragmentation potential includes the V_{LDM}, Proximity potential, Coulomb Potential and rotational energy components. Of course temperature and deformation orientation effects are included in DCM [4-12] potential. The idea of calculating α-decay branching ratios to the ground state rotational band of daughter nucleus is to investigate the effect of proximity potential along with extremely important angular momentum, deformation and orientation effects. It may be noted that the probability of residual daughter nucleus(in excited state) and the probability of α-transition from ground state of parent nucleus to the excited states of daughter nucleus is taken from reference [3]. However the preformation probability (in PCM) and penetrability are calculated using DCM [4-12] approach. The advantage of DCM approach is that the availability of preformation factor allows one to look out for probability of formation of various possible fragments at the compound nucleus state. We have done two sets of calculations in the first part we have calculated the α-decay branching ratios to the rotational band of ground state of daughter nuclei formed in the decay of ^{238}Pu, ^{242}Cm and ^{246}Cf nuclear systems within the Unified fission approach i.e. by taking preformation probability of α-fragment equal to 1. In the second approach we took preformed cluster model into account and put appropriate values of preformation probabilities into calculations. In both the cases Penetrability of α-fragment is calculated using WKB approximation. The result of Unified fission approach are shown in tables 3.1 - 3.3 and that of Preformed cluster approach in tables 3.4 – 3.6.

The α-decay branching ratios of the even-even nuclei i.e. ^{238}Pu, ^{242}Cm and ^{246}Cf to the ground state rotational band of their daughter nuclei calculated using the unified fission approach are shown in the tables 3.1, 3.2 and 3.3 respectively.

Table 3.1 Experimental and calculated α-decay branching ratios from the ground state of ^{238}Pu to the ground state rotational band of ^{234}U.

Rotational levels of daughter nuclei	Excitation energy of the rotational levels of daughter nuclei (MeV)	Branching Ratios, $b_{\ell+}$% (calc.) at T=0MeV	Branching Ratios, $b_{\ell+}$% (calc.) at T=1MeV	Branching Ratios, $b_{\ell+}$% (expt.)
0^+	0.000	72.80%	72.70%	70.91%
2^+	0.043	25.00%	25.06%	28.98%
4^+	0.143	2.093%	2.097%	0.105%
6^+	0.296	0.040%	0.040%	0.003%
8^+	0.497	3.2×10^{-4}%	3.2×10^{-4}%	6.8×10^{-6}%

Table 3.2 Experimental and calculated branching α-decay branching ratios from the ground state of ^{242}Cm to the ground state rotational band of ^{238}Pu.

Rotational levels of daughter nuclei	Excitation energy of the rotational levels of daughter nuclei (MeV)	Branching Ratios, $b_{\ell+}$% (calc.) at T=0MeV	Branching Ratios, $b_{\ell+}$% (calc.) at T=1MeV	Branching Ratios, $b_{\ell+}$% (expt.)
0^+	0.000	73%	73%	74%
2^+	0.044	24.6%	24.6%	25%
4^+	0.146	1.9%	1.9%	0.035%
6^+	0.303	0.03%	0.03%	0.003%
8^+	0.513	2.15×10^{-4}%	2.15×10^{-4}%	2.1×10^{-4}%

Table 3.3 Experimental and calculated α-decay branching ratios from the ground state of ^{246}Cf to the ground state rotational band of ^{242}Cm.

Rotational levels of daughter nuclei	Excitation energy of the rotational levels of daughter nuclei (MeV)	Branching Ratios, $b_{\ell+}$% (calc.) at T=0MeV	Branching Ratios, $b_{\ell+}$% (calc.) at T=1MeV	Branching Ratios, $b_{\ell+}$% (expt.)
0^+	0.000	72%	72.2%	79.3%
2^+	0.042	25.3%	25.3%	20.6%
4^+	0.138	2.3%	2.3%	0.150%
6^+	0.284	0.03%	0.06%	0.016%

One may note that α-branching ratios to the ground state rotational bands of respective daughters find nice comparison with the experimental data. The hindrance of the higher rotational band states is clearly evident. Interestingly the α-branching ratios seem to have negligible dependence on temperature and the α-branching ratios in tables 3.1 - .3.3 seem to be almost identical at T=0 and 1 MeV.

Further, the α-decay branching ratios of the even-even nuclei i.e. ^{238}Pu, ^{242}Cm and ^{246}Cf to the ground state rotational band of their daughter nuclei calculated using the Preformed cluster approach can be seen from the tables 3.4, 3.5 and 3.6 respectively.

Table 3.4 Experimental and calculated α-decay branching ratios from the ground state of ^{238}Pu to the ground state rotational band of ^{234}U.

Rotational levels of the daughter nuclei	Excitation energy of the rotational levels of daughter nuclei (MeV)	Branching Ratios, $b_{\ell+}$% (calc.) at T=0MeV	Branching Ratios, $b_{\ell+}$% (calc.) at T=1MeV	Branching Ratios, $b_{\ell+}$% (expt.)
0^+	0.000	72.7%	72.7%	70.91%
2^+	0.043	25.05%	25.09%	28.98%
4^+	0.143	2.10%	2.10%	0.105%
6^+	0.296	0.04%	0.04%	0.003%
8^+	0.497	3.25×10^{-4}%	3.25×10^{-4}%	6.8×10^{-6}%

Table 3.5 Experimental and calculated α-decay branching ratios from the ground state of ^{242}Cm to the ground state rotational band of ^{238}Pu.

Rotational levels of the daughter nuclei	Excitation energy of the rotational levels of daughter nuclei (Mev)	Branching Ratios, $b_{\ell+}$% (calc.) at T=0MeV	Branching Ratios, $b_{\ell+}$% (calc.) at T=1MeV	Branching Ratios, $b_{\ell+}$% (expt.)
0^+	0.000	73.0%	73.4%	74.0%
2^+	0.044	24.6%	24.6%	25.0%
4^+	0.146	1.9%	1.9%	0.035%
6^+	0.303	0.03%	0.03%	0.003%
8^+	0.513	2.1×10^{-4}%	2.17×10^{-4}%	2.1×10^{-5}%

Table 3.6 Experimental and calculated α-decay branching ratios from the ground state of ^{246}Cf to the ground state rotational band of ^{242}Cm.

Rotational levels of daughter nuclei	Excitation energy of the rotational levels of daughter nuclei (MeV)	Branching Ratios, $b_{\ell+}$% (calc.) at T=0MeV	Branching Ratios, $b_{\ell+}$% (calc.) at T=1MeV	Branching Ratios, $b_{\ell+}$% (expt.)
0^+	0.000	73.6%	72.2%	79.3%
2^+	0.042	24.16%	25.4%	20.6%
4^+	0.138	2.18%	2.29%	0.150%
6^+	0.284	0.03%	0.06%	0.016%

The results of Unified fission model and Preformed cluster model seem to compare experimental data quite nicely. Very slight deviations are observed with Preformed cluster approach when compared with UFM which indicate that probability of formation of α in chosen reaction is almost unity discarding the possibility of formation of any other cluster in decay of these nuclear systems. However even if the preformation probability of other fragments is significant, it might not make much effect in the calculation of branching ratios.

The systematic calculation of α-decay branching ratios to the rotational band is rare because some data of the excited states have been observed recently. The α-decay branching ratios to the excited states of even-even nuclei are calculated using both Unified fission approach and Preformed cluster approach. The results obtained for both the approaches seem to be equally good.

Experimentally it is known that the ground states of the even-even actinides mainly decay to the 0^+ and 2^+ states of the daughter nuclei. The sum of the branching ratios to the 0^+ and 2^+ states is as large as 99% in many cases.

The α-transition to other members of the rotational band are strongly hindered. It is evident from the tables above that the calculated values agree with the experimental ones both for low-lying states (0^+,2^+) and the high-lying ones (6^+,8^+), however the calculated branching ratio to the 4^+ state is slightly larger than the experimental one.

It would be very interesting to pursue this by performing more realistic calculations in the vicinity of 4^+ state. Nevertheless, the overall agreement of the branching ratios to the rotational band of the nuclei are largely acceptable.

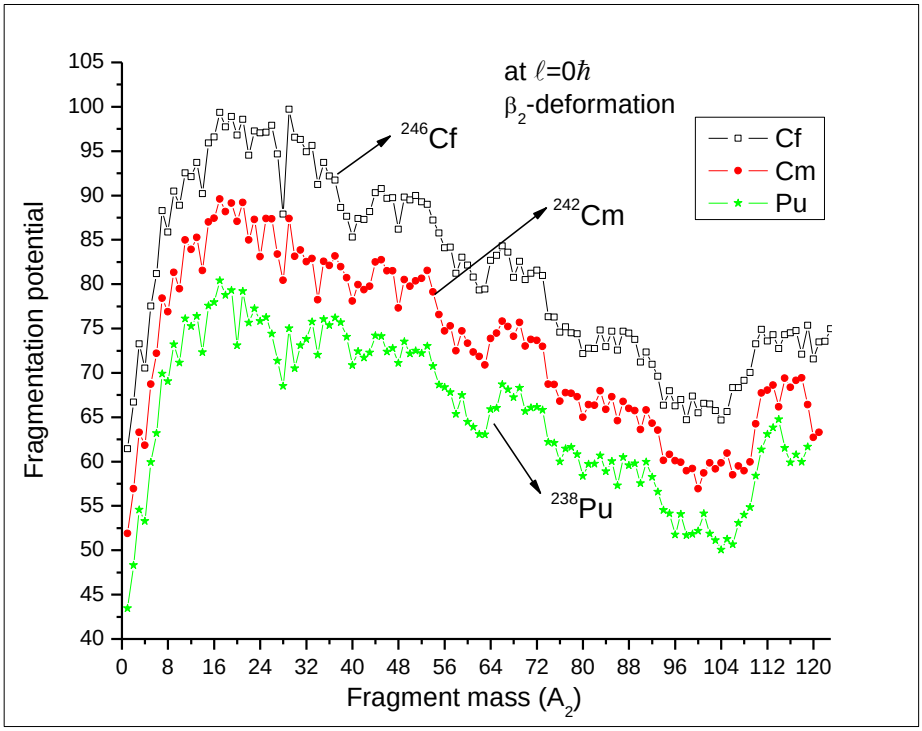

Figure 3.1 Fragmentation potential as a function of fragment mass for Pu, Cm and Cf.

Fig 3.1 shows the fragmentation potential as a function of fragment mass for Pu, Cm and Cf nuclear systems. The α-nucleus structure is quite evident in all the cases. At ℓ=0, the ER part seem to contribute more as compared to fission

fragments. However the trend may reverse at fairly large values of angular momentum.

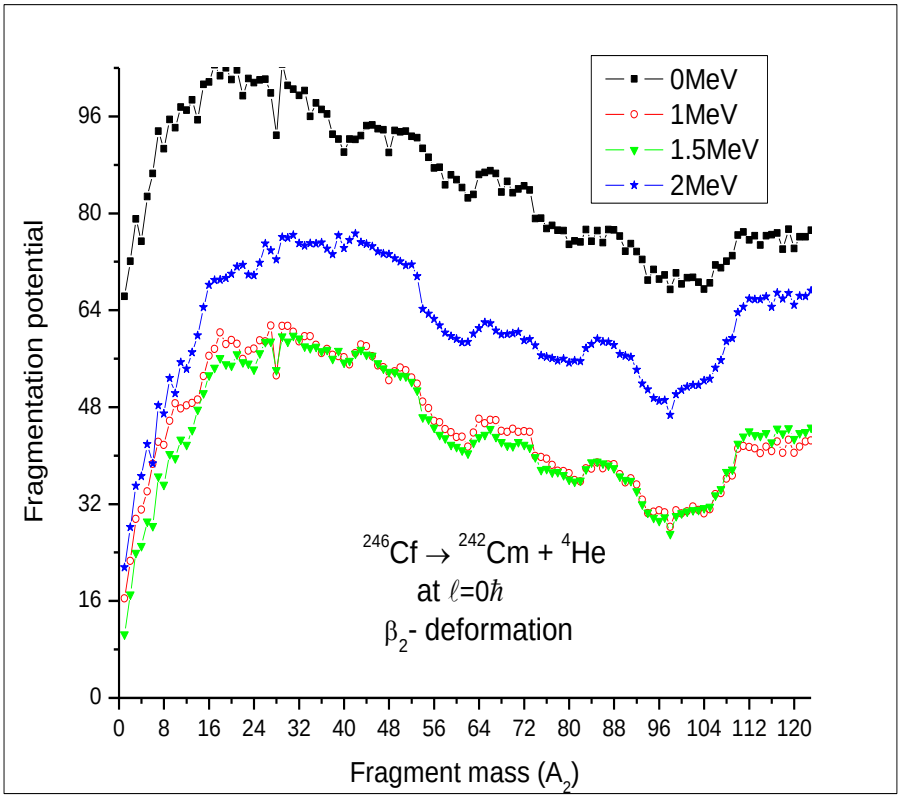

Figure 3.2 Fragmentation potential as a function of fragment mass A_2.

Fig 3.2 shows the temperature dependence on the fragmentation potential for the decay of ^{246}Cf. Although overall behavior remain similar over a variation of 2 MeV but the α-nuclear structure seen to vanish beyond T=1 MeV, as expected.

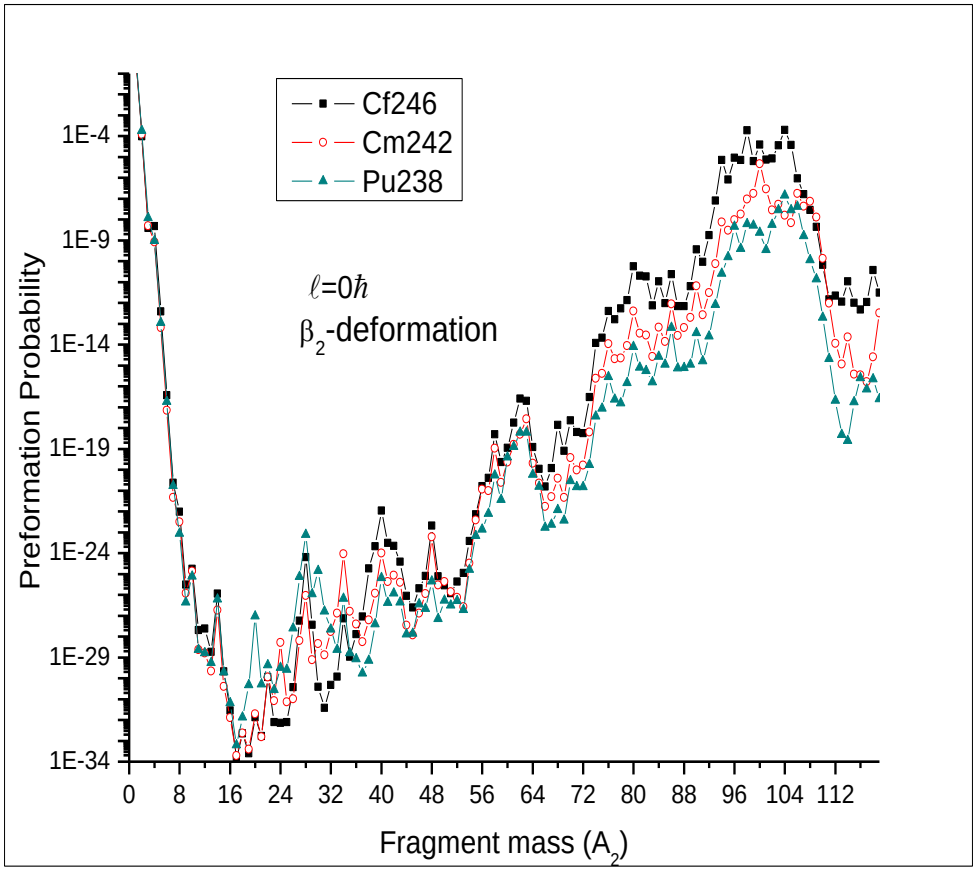

Figure 3.3 Preformation probability as a function of fragment mass for ^{246}Cf, ^{242}Cm and ^{238}Pu.

Fig 3.3 depicts the preformation probability as a function of fragment mass for ^{238}Pu, ^{242}Cm and ^{246}Cf. It is relevant to mention here that preformation probability is the probability of formation of fragment in the compound nucleus state and it provides the much needed structure information of the nucleus under investigation. The fragmentation path for all the three nuclei considered here is quite identical and a near asymmetric fission kind of fragmentation is predicted for three of them.

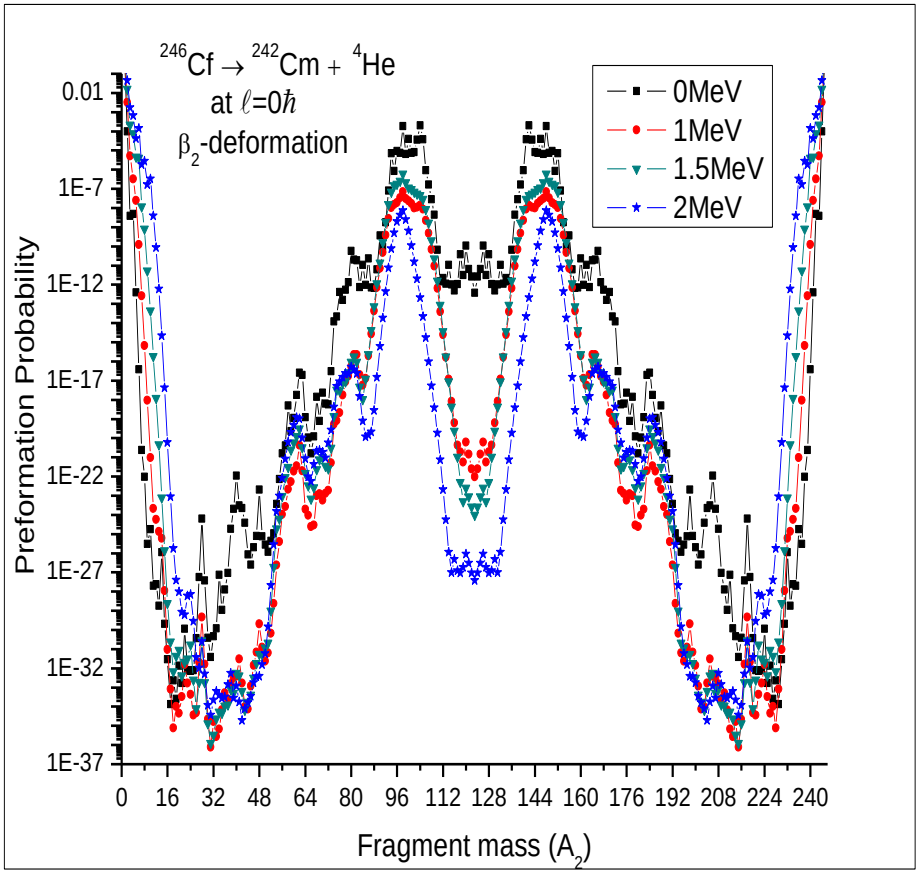

Figure 3.4 Preformation probability as a function of fragment mass A_2 at different temperatures.

Temperature dependence on Preformation probability is shown in fig 3.4. Not much difference is seen in the potential energy surfaces (PES) over a wide range of temperature and fragment distribution remain asymmetric in nature throughout.

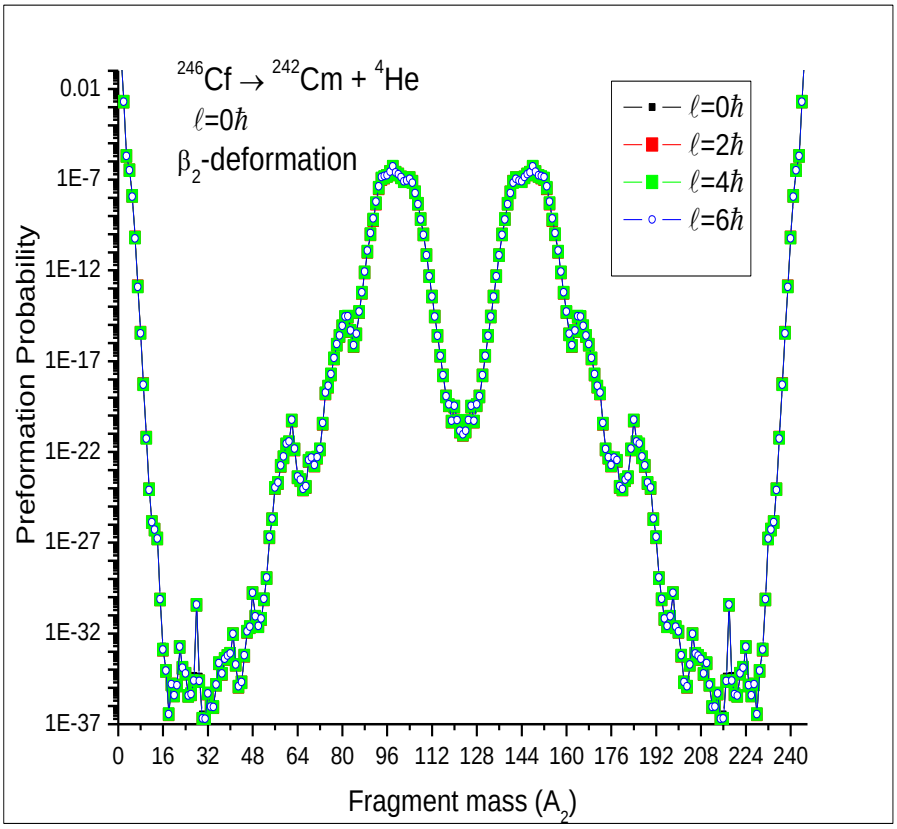

Figure 3.5 Preformation probability as a function of fragment mass A_2.

The figure 3.5 is the plot between preformation probability and fragment mass (A_2) at T=1MeV at angular momentum 0^+, 2^+, 4^+ and 6^+ states of the ground state rotational band of ^{242}Cm. As is evident from the figure, the preformation probability for different values of angular momentum are same for a given temperature. That means preformation probability is almost identical/same for various rotational bands investigated in this work. This might be another reason that UFM and PCM don't show much deviation in their result. However, it might be interesting to investigate the role of higher values of angular momentum in the α-decay of ^{246}Cf nucleus.

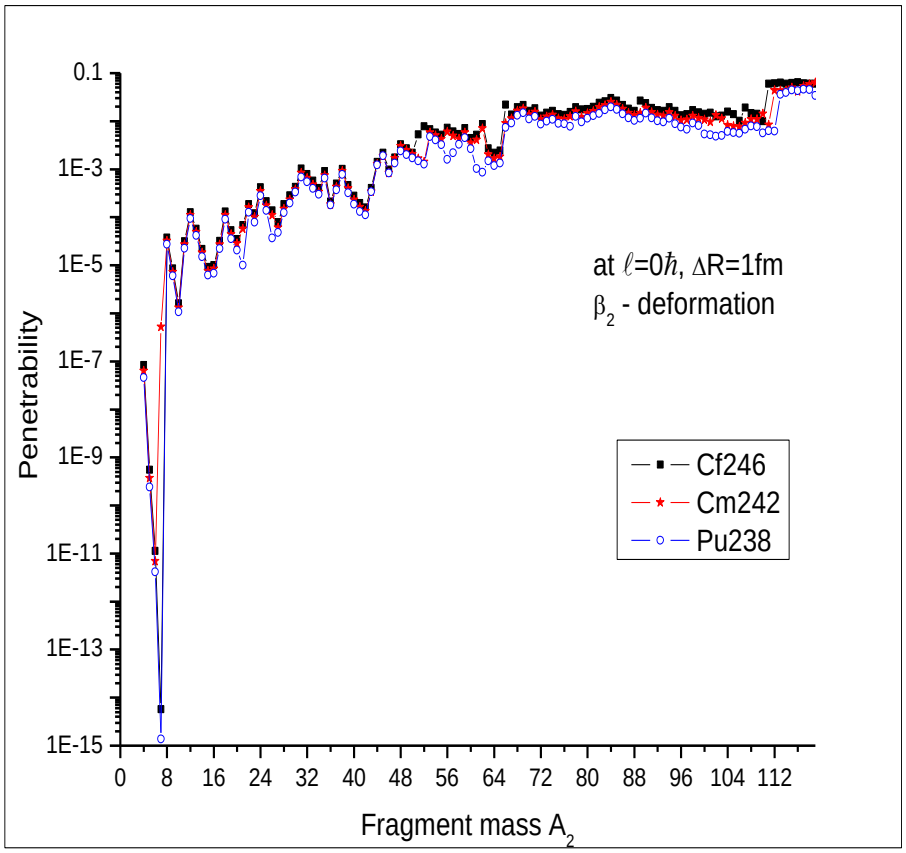

Figure 3.6 Penetrability as a function of fragment mass A_2.

The penetration probability of ^{238}Pu, ^{242}Cm and ^{246}Cf is shown in the figure 3.6. Interestingly the penetration behavior of Pu, Cm and Cf look quite similar.

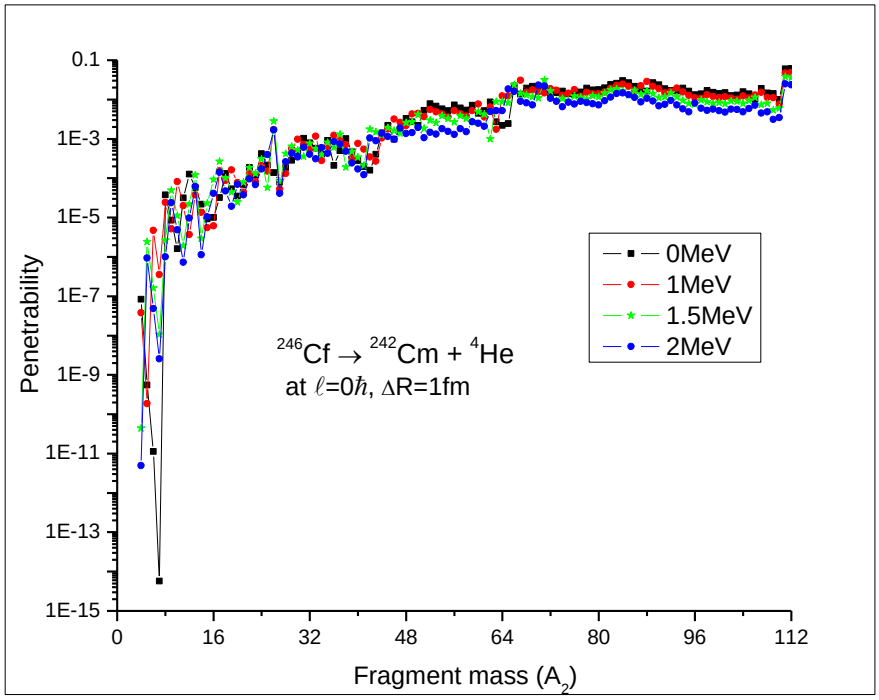

Figure 3.7 Penetration probability as a function of fragment mass at different temperatures.

The temperature dependence of penetrability studied in the figure 3.7. Although we observe significant variation at higher temperature for fragments less than 16, but for remaining fragments the temperature doesn't seem to influence the penetration probability much and the variation seems almost similar for fragments with A_2> 16.

In summary, the α-decay branching ratios of even-even nuclei have been calculated in the framework of DCM by taking into account the angular momentum of the α-particle and the excitation probability of the daughter nucleus. The calculated branching ratio to the rotational band of the ground state of the even-even actinides are consistent with the experimental data except for the branching ratios to the 4^+ state with UFM as well as PCM. The dependence of potential energy surfaces on temperature and angular momentum is also addressed. The present set of calculations reveal some interesting information regarding the nuclear structure and related aspects.

REFERENCES

[1] G.Gamow, Z. Phys. **51**, 204 (1928)

[2] E.U.Condon and R.W.Gurney, Nature (London) **122**, 439 (1928)

[3] Y.Z.Wang, H.F.Zhang, J.M.Dong, G.Royer, Phys. Rev. C **79**, 014316 (2009)

[4] R.K. Gupta, M. Balasubraniam, C. Mazzocchi, M. La Commara, and W. Scheid, Phys. Rev. C **65**, 024601 (2002).

[5] M.K. Sharma, R.K. Gupta, and W. Scheid, J. Phys. G **26**, L45 (2000).

[6] R.K. Gupta, R. Kumar, N.K. Dhiman, M. Balasubraniam, W. Scheid, and C. Beck, Phys. Rev. C **68**, 014610 (2003).

[7] M. Balasubraniam, R. Kumar, R.K. Gupta, C. Beck, and W. Scheid, J. Phys. G **29**, 2703 (2003).

[8] R.K. Gupta, M. Balasubraniam, R. Kumar, D. Singh, and C. Beck, Nucl. Phys. A **738**, 479c (2004).

[9] R.K. Gupta, M. Balasubramaniam, R. Kumar, D. Singh, C. Beck, and W. Greiner, Phys. Rev. C **71**, 014601 (2005).

[10] B.B. Singh, M.K. Sharma, R.K. Gupta, and W.Greiner,Int.J. Mod.Phys.E15, 699 (2006)

[11] R.K. Gupta, M. Balasubraniam, R.Kumar, D.Singh ,S.K. Arun and W.Greiner,J.Phys .G:Nucl.Part. Phys. **32**, 345(2006)

[12] B.B. Singh, M.K. Sharma, R.K. Gupta,Phys.Rev. C **77**, 054613 (2008)